CleanMat

WILEY

CleanMat

RESEARCH ARTICLE OPEN ACCESS

Implementation of a Packed Bed Reactor With Mycological Silver Nanoparticles for Drinking Water Disinfection

Ana Laura Pires de Oliveira[1,2] | Stella Daniels Kovacs[1,2] | Carolina Assis da Silva[1,2] | Caterina do Valle Trotta[1,2] | Marta Filipa Simões[3,4] | Rafael Firmani Perna[5] | Cristiane Angélica Ottoni[1,6]

[1]São Paulo State University (UNESP), Institute of Biosciences, São Vicente, Brazil | [2]São Paulo State University (UNESP), Institute of Advanced Studies on Ocean, São Vicente, Brazil | [3]State Key Laboratory of Lunar and Planetary Sciences (SKLPlanets), Macau University of Science and Technology (MUST), Taipa, China | [4]China National Space Administration (CNSA), Macau Center for Space Exploration and Science, Taipa, China | [5]Federal University of Alfenas, Institute of Science and Technology, Poços de Caldas, Brazil | [6]LEAF-Linking Landscape, Environment, Agriculture and Food Research Center, Associated Laboratory TERRA, Instituto Superior de Agronomia, Universidade de Lisboa, Lisboa, Portugal

Correspondence: Cristiane Angélica Ottoni (cristiane.ottoni@unesp.br)

Received: 13 March 2025 | **Revised:** 8 August 2025 | **Accepted:** 10 August 2025

Funding: The research described in this work was supported by the São Paulo Research Foundation (FAPESP; grant # 2020/12867-2). CAO acknowledges support from the Conselho Nacional de Desenvolvimento Científico e Tecnológico (CNPq; grants #421122/2023-4 and #313031/2025-8). RFP thanks Minas Gerais Research Foundation (FAPEMIG #APQ-00085-21; #BPD-00030-22) and CNPq (grant #404912/2021-4). MFS was supported by the Science and Technology Development Fund (FDCT), Macau SAR, China (Files No. 0033/2024/ITP1 and 002/2024/SKL) and the National Key Research and Development Program of China (Grant No. 2022YFE0204600). CAS acknowledges scholarships financial support from FAPESP #23/08202-3; #22/05716-3, and #22/03562-9. CVT and ALPO acknowledge scholarships financial support from Coordination for the Improvement of Higher Education Personnel (CAPES # 88882.469336/2019-01 and #88887.822485/2023-00). SK thanks the financial support from CNPq scholarship (114290/2023-7).

Keywords: calcium alginate | *Escherichia coli* | packed-bed reactor | silver myconanoparticles | water disinfection

ABSTRACT

Basic sanitation and access to drinking water are critical challenges for developing countries. By 2025, water scarcity could affect 50% of the global population. Given this scenario, the search for sustainable and cost-effective water purification methods has driven research into the application of biologically synthesized silver nanoparticles (AgNPs). In this study, AgNPs were produced using the filamentous fungus *Aspergillus niger* IBCLP20 and encapsulated in calcium alginate ($AgNP_{IBCLP20/CA}$) for use in a packed-bed reactor (PBR) to treat water contaminated with *Escherichia coli* IPT245 and *Pseudomonas aeruginosa* IPT365. To evaluate the process parameters for water disinfection, the following variables were assessed: influent bacterial concentration (10^3, 10^4, and 10^5 CFU·mL^{-1}), temperature (25°C, 30°C, 37°C, and 40°C), reactor occupancy (50%, 75%, and 100%), and volumetric feed flow rate (1.0, 4.0, 7.0, and 10.0 mL·min^{-1}). In the experiments, *P. aeruginosa* IPT365 exhibited greater resistance compared to *E. coli* IPT245. For both bacteria, the best antimicrobial results were obtained at an influent concentration of 10^3 CFU·mL^{-1}. Temperature had no significant impact on the system for either of the bacterial strain. The antimicrobial activity against *E. coli* IPT245 was observed for all reactor occupancy levels tested, whereas the bactericidal effect against *P. aeruginosa* IPT365 was only achieved when the PBR was filled to 100% of the catalyst mass. The optimum volumetric flow rate was determined to be 4.0 mL·min^{-1}. These findings confirm that the PBR with encapsulated $AgNP_{IBCLP20/CA}$ is a promising approach for water disinfection. The maintenance of antimicrobial activity after nanoparticle encapsulation, along with a detailed analysis of operational parameters, supports the feasibility of this method for environmental applications.

1 | Introduction

Drinking water contamination by *Escherichia coli* is a global concern, often linked to outbreaks of waterborne diseases. The presence of these microorganisms in water highlights the significant health risks, especially in regions with inadequate sanitation systems. In these areas, poor sanitation often leads to contaminated water sources, which in turn contributes to higher infant mortality rates. Access to clean water and proper sanitation is critical for preventing such contamination and the diseases associated with it [1]. *Pseudomonas aeruginosa* is a Gram-negative bacterium that can be found in varying places, including water, soil and hospital surfaces. This bacterium can cause serious infections, such as pneumonia, urinary tract infections and septicemia, and its presence in drinking water poses a great threat to public health [2].

Packed-bed reactors (PBR) operate with solid particles or immobilized catalysts that promote chemical and biological reactions, that allow the removal of contaminants in a continuous process [3, 4]. The main advantage of PBR consists in the maximized contact between the fluid to be treated and the support particles [5]. This technology not only allows for the treatment of large volumes of water, but also presents lower operational and maintenance costs when compared to more complex systems, such as photoreactors [6], enabling easier industrial scale amplification [7]. The simplicity of construction and the scalability of these reactors (PBR) are factors that make them interesting to apply in regions where financial and technological resources are limited [8].

Nanomaterials (NM) have been highlighted as a promising research field, notably in the biomedicine and the materials science fields. Between them, silver nanoparticles (AgNPs) are amply recognized for their antibacterial properties, applicable against various pathogens [9, 10]. AgNPs can be obtained from chemical methods, which utilize commercial reagents, and physical methods, by the decomposition of material, as well as by biological synthesis, that employ natural reducing agents, including bacteria, filamentous fungi or plants [11, 12]. Recent studies have demonstrated that synthetic AgNPs can present good applicability due to the antibacterial properties of the NM, but biological AgNPs exhibits additional advantages, namely lower environmental toxicity and higher biocompatibility [13]. Furthermore, the uniformity in size and shape of AgNPs produced through biological processes makes them especially advantageous for water treatment purposes [14, 15].

Filamentous fungi (Ff) are promising organisms for NP biological synthesis, due to their easy laboratory maintenance and easy cultivation [16]. Besides that, these microorganisms have high tolerance and capacity to reduce metals, including heavy metals, to the nanometric scale. Those NP present higher biocompatibility in comparison with commercial NP [17, 18]. Extracellular synthesis of AgNPs by *Ff* involves exposing the fungal filtrate to silver nitrate ($AgNO_3$) solution, generating basic silver (Ag^0) in nanometric scale [19]. The antibacterial action of AgNPs is attributed to the release of silver ions (Ag^+), that interact directly with bacterial cell membranes and their DNA, thus resulting in the microorganism's death [20, 21].

Furthermore, the utilization of encapsulated AgNPs in non-toxic compounds, for example alginate, utilized as encapsulation agent [22, 23] and applied as filling in a PBR for drinking water treatment in a continuous process, is an innovative and promising alternative to the conventional established methods, with the possibility of reducing agglomeration and controlling silver ions release, potentiating its antibacterial properties against potentially pathogenic bacteria such as *Escherichia coli* and *P. aeruginosa* [24]. In short, mycological AgNPs produced by Ff and encapsulated in calcium alginate, utilized in a PBR, present a promising alternative to disinfect water contaminated by pathogenic bacteria.

2 | Materials and Methods

2.1 | Myconanoparticles Encapsulation

The *Aspergillus niger*$_{IBCLP20}$ strain was acquired from the Culture Collection of the Biosciences Institute, São Paulo State University (UNESP), Brazil. The protocol of AgNPs synthesis was previously described by Silva et al. (2022) [13]. According to Silva et al. (2022) [13], $AgNP_{IBCLP20}$ possess spherical shape size ranging of 37.4–67.4 nm measured by transmission electron microscope (TEM), 80.50 ± 8.77 nm by Dynamic light scattering (DLS), zeta potential (Pζ) −38.56 and Polydispersity index (PDI) of 0.215.

The microcapsules were obtained by ionotropic gelation with sodium alginate according to data described in the literature [25]. The biopolymer solution was prepared by solubilizing 3.1% (w/v) sodium alginate in 10 mL of biological AgNPs. Subsequently, the biopolymer solution (10 mL) was dripped into 100 mL of an aqueous calcium chloride solution (0.14 M) using a 20 mL intravenous infusion syringe and a 27g intravenous infusion device [26]. The system was kept under constant magnetic stirring (500 rpm) for 1 min. After the gelling process, the microcapsules were vacuum filtered and stored at 4°C.

2.2 | Reactor Parameters

The packed bed reactor (PBR) (Figure 1) was made of borosilicate glass with a nominal diameter and length of 1.2 and 20 cm, respectively. The bed was filled to 100% (17.5 g), 75% (13.125 g) or 50% (8.75 g), weighed on an analytical balance (Sigma-Aldrich), with (a) fungal $AgNP_{IBCLP20}$ encapsulated in calcium alginate ($AgNP_{IBCLP20/CA}$); (b) $AgNO_3$ encapsulated in calcium alginate as a positive control ($AgNO_{3/CA}$); (c) calcium alginate (CA), and (d) glass beads (GB) as negative controls. The bed was 100% filled with 25 sterile glass beads at the bottom, 17.5 g of encapsulated material and 35 sterile glass beads at the top. The glass beads act as anchors to keep the calcium alginate beads (which encapsulate AgNPs and $AgNO_3$) fixed in place within the reactor. This prevents them from floating freely or aggregating, which could disrupt flow dynamics or reduce exposure to nutrients.

The influent (water contaminated with potentially pathogenic bacteria, *E. coli* IPT245 or *P. aeruginosa* IPT365) was fed to the reactor in a water bath at an optimum temperature of 37°C and flowed upwards through a silicone pipe (0.5 cm in diameter) to the inlet of the PBR reactor using a peristaltic pump. Samples (effluent) were collected every hour from the top outlet of the PBR reactor for a period of 8 h, in triplicate. The effluent samples were analyzed by counting colonies grown on plates with Trypticase Soy Agar (TSA) final composition (g/L): agar (15.0) (Exodo), bacteriological peptone (15.0) (Exodo), soy peptone (5.0) (Himedia), sodium chloride (5.0) (Exodo), after 24 h. The temperature of the process was controlled in the reactor by a thermal jacket circulating water from a thermostatic bath. The ends (inlet and outlet) of the reactor were fitted with distribution trays machined from Teflon material in order to homogenize the radial dispersion of the influent through the reactor bed.

2.3 | Antimicrobial Mycogenic Nanoparticles Activities

To implement the continuous process for disinfecting contaminated water, the following parameters were evaluated: influent concentration (10^3, 10^4, and 10^5 CFU·mL^{-1}), temperature (25°C, 30°C, 37°C, and 40°C), reactor occupancy (50%, 75%, and 100%), and volumetric feed flow rate (1.0, 4.0, 7.0, and 10.0 mL·min^{-1}), the latter based on parameters used in previous studies by our group. The parameters of 10^3 CFU·mL^{-1}, 37°C, 100% reactor occupancy (17.5 g), and a volumetric feed flow rate of 4.0 mL·min^{-1} were established as standard conditions, with variations applied to the evaluated parameter.

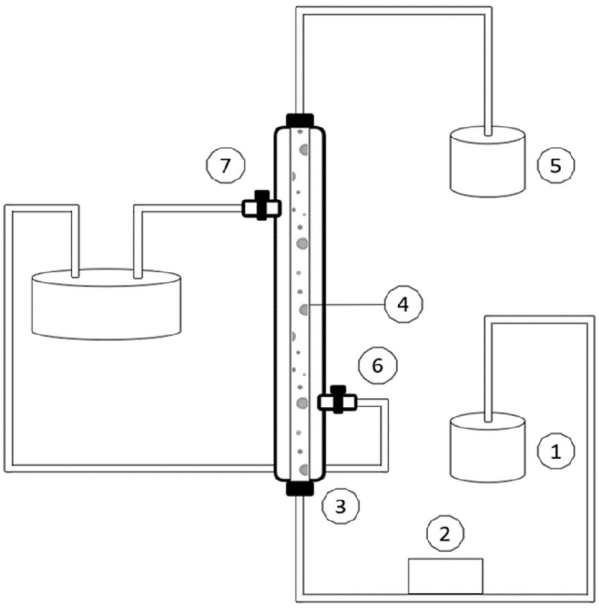

FIGURE 1 | Packed-bed reactor (PBR) structure: (1) Influent; (2) Peristaltic pump; (3) Influent entrance; (4) Packed-bed reactor (PBR) filled with (CA, $AgNP_{IBCLP20/CA}$, $AgNO_{3/CA}$, GB); (5) Sample retrieval (effluent); (6) Water bath entrance; (7) Water bath exit. $AgNP_{IBCLP20/CA}$ = silver nanoparticles produced using the filamentous fungus *Aspergillus niger* IBCLP20 and encapsulated in calcium alginate; $AgNO_{3/CA}$ = silver nitrate encapsulated in calcium alginate; CA = calcium alginate; GB = glass beads.

2.4 | Data Analysis

The antibacterial activity of the compounds was statistically analyzed according to the United States Environmental Protection Agency (USEPA) (2002) [27] in the GraphPad Prism software v10.1.1 (270), using the *t*-test, after previously evaluating the assumptions of normality using the Shapiro Wilk test and homoscedasticity using the F test. Tukey's test with a 95% confidence interval was also used to analyze pairs of means.

3 | Results and Discussion

3.1 | Mycogenic AgNPs Encapsulation in Calcium Alginate

The characterization of nanomaterials is crucial for their biotechnological applicability and for validating the methodology used during the synthesis process. This is because physicochemical characteristics such as morphology, size, and charge can significantly influence their properties [28]. In colloidal solution, the hydrodynamic size of $AgNP_{IBCLP20}$ was 80.50 ± 8.77 nm whereas TEM characterization revealed nanoparticle sizes ranging from 37.4 to 67.4 nm [13]. Since TEM directly measures the solid nanomaterial, it determines the core size with greater precision at the nanometric scale [12, 19]. Figure 2 shows the mycogenic $AgNP_{IBCLP20}$ encapsulated in calcium alginate ($AgNP_{IBCLP20/CA}$). One $AgNP_{IBCLP20/CA}$ weighing ≅ 40 mg and with an average diameter of 3 mm.

The size distribution of NP, measured by the Polydispersity Index (PDI), classifies the particles as monodisperse when the obtained value is closer to 0, and polydisperse when the values are close to 1.0. The AgNPs used in this study had an index of 0.215, and thus, they were classified as monodisperse. Another important parameter evaluated was the zeta potential (Pζ), which indicated a value of −38.56 mV for the biological nanomaterial [13]. Pζ is an indicator of the chemical stability of the NP, and by definition, values higher than +30 mV or lower than −30 mV are considered indicative of greater stability. The stability of the NPs is compromised by physical interactions that trigger aggregation, thus altering their size [29]. Biologically synthesized NPs are stabilized by biomolecules that reduce their tendency to aggregate, thereby increasing their stability [21, 28–30]. Accordingly, mycogenic AgNPs exhibit improved stability and a lower likelihood of agglomeration due to charge-based repulsion mechanisms [12, 19].

FIGURE 2 | Mycogenic silver nanoparticles (AgNPs) encapsulated in calcium alginate (CA) beads with a medium diameter of 4 mm.

Additionally, the encapsulation of NPs such as AgNPs prevents agglomeration and allows for their reuse [31]. The results indicate that the $AgNP_{IBCLP20/CA}$ have a silver content of 92 $mg{\cdot}L^{-1}$, an average concentration obtained by evaluating five spheres. Although ED-XRF (Energy Dispersive x-ray Fluorescence) provides reliable and non-destructive analysis, its ability to distinguish between metallic and ionic forms of silver is limited [32, 33]. This means that the presence of silver in the colloidal solution may include both AgNPs and silver ions (Ag^+), and additional methods are required for a more detailed evaluation of the dissolution of AgNPs into Ag^+ ions.

However, the use of encapsulated AgNPs, especially in materials such as alginate, appears promising in disinfection processes, as its encapsulation can help control the release of Ag^+ ions, reducing the potential harm of dispersed AgNPs. This approach also preserves the properties of AgNPs over long periods, enabling their repeated use [24, 34]. Given that the toxicity of AgNPs is closely associated with their size, shape, and surface contact area [13, 35, 36], maintaining these characteristics is essential for ensuring both effectiveness and safety in various applications.

The negative control, composed of CA, maintained the initial bacterial cell density throughout the tests, confirming the non-toxic nature of the encapsulating agent against the potentially pathogenic strains *E. coli* IPT245 and *P. aeruginosa* IPT365. This corroborates previous studies described by Alavi and Rai [24], which highlight the biocompatibility of the polymer and its low toxicity. Additionally, Ching and Bhandari [37], along with Kumar et al. [38], emphasized other important characteristics associated with alginate, such as biodegradability and greater stability. Consequently, the use of the encapsulated material did not compromise bacterial survival and did not alter the functionality of the AgNPs [26].

3.1.1 | Effluent Density

Figure 3 A.1 and 3 B.1 show that $AgNP_{IBCLP20/CA}$ exhibited a bactericidal effect on both *E. coli* IPT245 and *P. aeruginosa* IPT365, demonstrating the NPs applicability over an 8-h exposure period. At a cell density of 10^4 $CFU{\cdot}ml^{-1}$, $AgNP_{IBCLP20/CA}$ showed stronger antibacterial activity against *E. coli* IPT245 (Figure 3 A.2) compared to *P. aeruginosa* IPT365 (Figure 3 B.2). In Figure 3 (A.2), it can be seen that the NPs had a bactericidal effect after 1 h of exposure, and kept the bacteria *E. coli* bacteria with a cell density below 10^4 $UFC{\cdot}mL^{-1}$ in the remaining hours of sampling, 10^3 $UFC{\cdot}mL^{-1}$ in hours 2, 3, 4, and 8; and 10^2 $UFC{\cdot}mL^{-1}$ in 5, 6 and 7 h of sampling, $AgNO_{3/CA}$ kept the bacteria with densities at 10^3 $UFC{\cdot}mL^{-1}$ during the 8 h of the experiment, with statistical differences between both $AgNP_{IBCLP20/CA}$ and the precursor ($AgNO_{3/CA}$) in relation to the control.

At a density of 10^5 $UFC{\cdot}mL^{-1}$, both bacterial strains, *E. coli* IPT245 (Figure 3 A.3) and *P. aeruginosa* IPT365 (Figure 3 B.3), showed high survival rates regardless of the compound to which they were exposed. After 1 h of exposure, cell densities remained at 10^5 $CFU{\cdot}mL^{-1}$, except for $AgNO_{3/CA}$, where the bacteria had a cell density of 10^4 $CFU{\cdot}mL^{-1}$, thus being more toxic than bio-$AgNP_{AC}$. However, after 4 h of exposure, the cell density exceeded 10^6 $UFC{\cdot}mL^{-1}$ in both bacteria tested. Despite $AgNO_{3/CA}$ showing higher toxicity in the first hour, no statistical differences were observed between any of the compounds (CA, $AgNP_{IBCLP20/CA}$, $AgNO_{3/CA}$) and the control over the full duration of the experiment.

In alignment with our findings, AgNPs are known to disrupt multiple essential cellular processes in *P. aeruginosa*, including DNA replication, electron transport chain activity, signal transduction, and membrane integrity [39]. These effects are primarily driven by the generation of reactive oxygen species (ROS) and the release of silver ions, which induce oxidative stress and genotoxicity, ultimately compromising biofilm structure [40]. As emphasized by Lucky and Kusi (2025) [41], the physicochemical properties of surface coatings significantly influence the environmental behavior and antimicrobial efficacy of nanomaterials. These, together with our results show that coated AgNPs exhibit enhanced antimicrobial activity against *P. aeruginosa* compared to uncoated forms.

The encapsulating agent, CA, showed a statistically significant difference compared to the control made with glass beads (GB), likely due to biofilm formation on the GB surface. This biofilm formation may have contributed to a reduction in cell density to 10^3 $CFU{\cdot}mL^{-1}$ in the 6, 7, and 8 h samples, a behavior commonly found on *P. aeruginosa*, as cited in several studies [42, 43]. Additionally, biological reactors have a high potential for microorganisms adhesion, requiring appropriate cleaning procedures to remove biofilm formed [44]. Moreover, CA ($(C_{12}H_{14}CaO_{12})_n$) has a high carbon availability, which may have served as an energy source for the bacteria, leading to greater cell survival in the alginate compared to the control [45, 46].

3.1.2 | Temperature

According to Figure 4 A,B (1–4), at all evaluated temperatures, the microbial survival of both bacteria remained stable in the GB and CA controls. Meanwhile, $AgNP_{IBCLP20/CA}$ and $AgNO_{3/CA}$ sustained their bactericidal activity throughout the duration of the tests.

According to Ohshima et al. [47], although 37°C is considered optimal for many bacteria, these microorganisms exhibit significant tolerance to temperature variations. Studies report that 8°C allows only minimal bacterial survival, while 44°C represents the upper limit for exponential growth, and 50°C induces fragility in *E. coli* [48, 49]. Additionally, research suggests that the antibacterial activity of AgNPs are influenced by the temperature at which they are tested, with higher temperatures enhancing their antibacterial properties [50–52]. Although bacteria can adapt to temperature variations by incorporating more saturated fatty acids into their membrane phospholipids to maintain cellular integrity [47, 49] the antibacterial activity of $AgNP_{IBCLP20/CA}$ was observed across different temperatures. While elevated water temperatures increase the antibacterial efficacy of Ag^+ containing materials, other factors such as turbidity and pH can modulate their effects. Song et al. [51] and Zhang et al. [52] examined the influence of pH on antibacterial performance and found that higher temperatures reduce the time required for complete bacterial elimination. However, additional parameters must be

considered, as they can impact on the overall antibacterial efficiency of the compound. Therefore, further studies should be conducted to determine the optimal temperature for industrial applications, particularly when scaling up the process.

3.1.3 | Reactor Occupancy

A PBR reactor loaded with 8.75 g (50%), 13.125 g (75%), and 17.5 g (100%) of catalytic mass ($AgNP_{IBCLP20/CA}$) was used to evaluate the antibacterial efficiency against *E. coli* IPT245 and *P. aeruginosa* at a cell density of 10^3 CFU·mL^{-1}. Figure 5A illustrates that, with the reactors filled to 50% capacity (Figure 5 A.1), *E. coli* IPT245 exhibited an initial survival rate of 10^2 CFU·mL^{-1} within the first hour of the assay. However, the bactericidal efficiency reached 100% in the subsequent hours. In the cases of 75% (Figure 5 A.2) and 100% (Figure 5 A.3) filling, the bactericidal effect remained at 100% throughout the 8 h of operation. *P. aeruginosa* IPT365 proved to be more resistant when exposed to a lower amount of catalytic mass (Figure 5 B.1 and B.2), with cell survival of 10^2 CFU·mL^{-1} up to 3 h of exposure to $AgNP_{IBCLP20/CA}$ and up to 4 h when exposed to $AgNO_{3/CA}$, with a bactericidal effect only in the last hours of exposure to the compounds, which may have been due to the characteristic of CA in controlling the release of the encapsulated compound, thus having a lower amount of Ag^+ and $AgNP_{IBCLP20/CA}$ available [34, 53] As shown in Figure 5 B.3, the only condition in which the greatest antibacterial activity was obtained during the 8 h of exposure was when the reactor was operated at 100% filling.

Regarding the catalyst mass, several studies have examined the parameter of the amount of Ag^+ and available AgNPs in the medium, with Ag^+ concentrations ranging from 0.01% to 5% by weight [51, 52, 54–58]. Using different materials, some studies

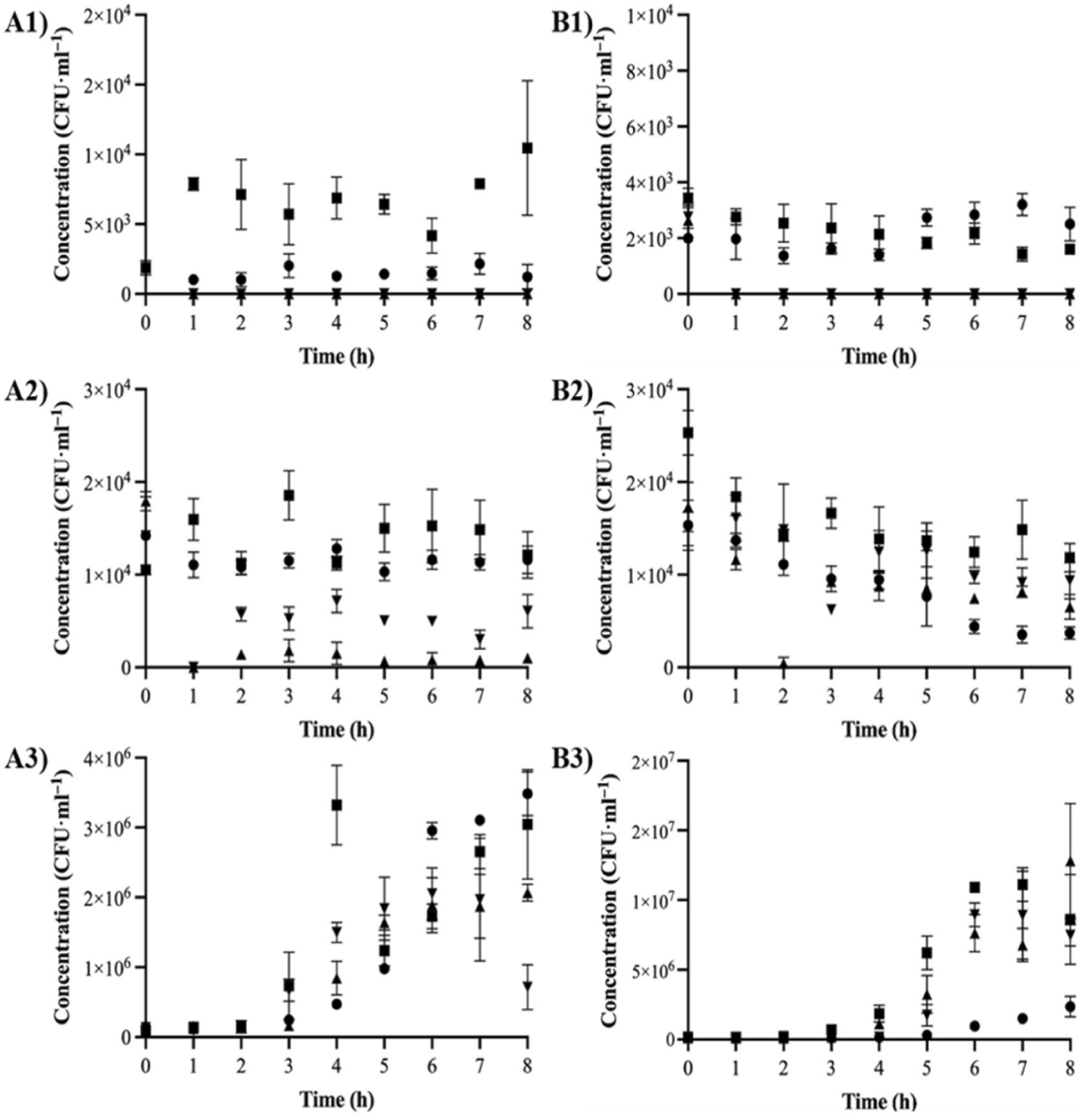

FIGURE 3 | Evaluation of the applicability of the packed bed reactor (PBR) filled to 100% with glass beads (GB) (●), calcium alginate (CA) (■), $AgNP_{IBCLP20/CA}$ (▲), or $AgNO_{3/CA}$ (▼) for the decontamination of (A) *Escherichia coli* IPT245 and (B) *Pseudomonas aeruginosa* IPT365. The reactor was operated at 37°C with a continuous flow rate of 4.0 mL·min^{-1}, and bacterial densities of (1) 10^3 CFU·mL^{-1}, (2) 10^4 CFU·mL^{-1}, and (3) 10^5 CFU·mL^{-1} were evaluated.

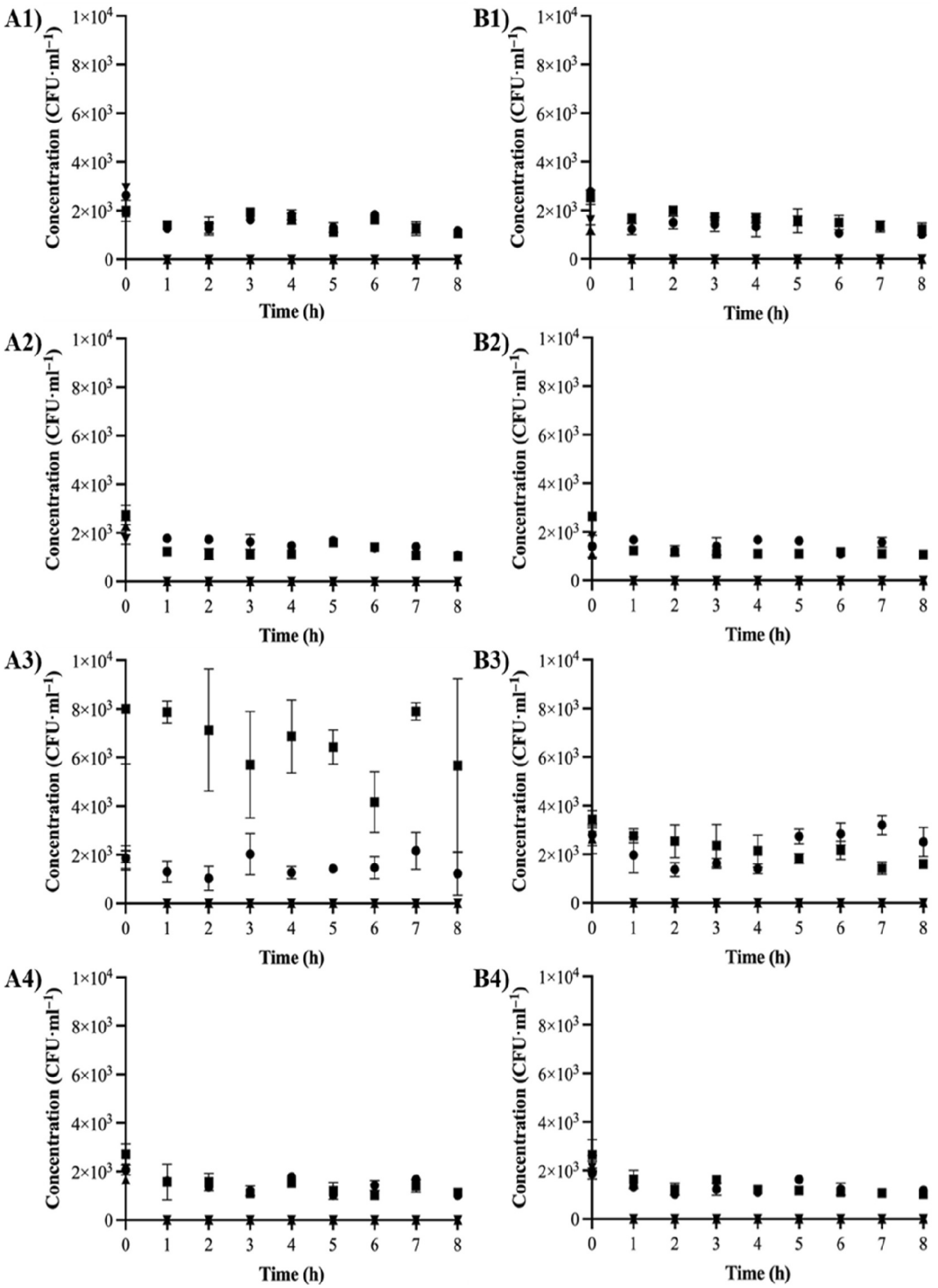

FIGURE 4 | Evaluation of the applicability of the packed bed reactor (PBR) filled to 100% with glass beads (GB) (●), calcium alginate (CA) (■), $AgNP_{IBCLP20/CA}$ (▲), or $AgNO_{3/CA}$ (▼) for the decontamination of (A) *Escherichia coli* IPT245 and (B) *Pseudomonas aeruginosa* IPT365. The reactor was operated at 25°C (1), 30°C (2), 37°C (3), and 40°C (4), with a continuous flow rate of 4.0 $mL \cdot min^{-1}$.

indicate that increasing the Ag^+ concentration did not significantly affect the diameters of the inhibition zones [56, 58], while others [54, 57] found that increasing the Ag^+ concentration led to larger inhibition zone diameters.

There are conflicting views on the effect of Ag^+ concentration on disinfection performance. Consequently, the relationship between Ag^+ concentration and disinfection rate need to be clarified, and the potential combined effects with other parameters require further exploration.

3.1.4 | Volumetric Feed Flow Rate

The volumetric flow rate was set to 1.0, 4.0, 7.0, and 10.0 $mL \cdot min^{-1}$ and monitored every 30 min throughout the 8-h

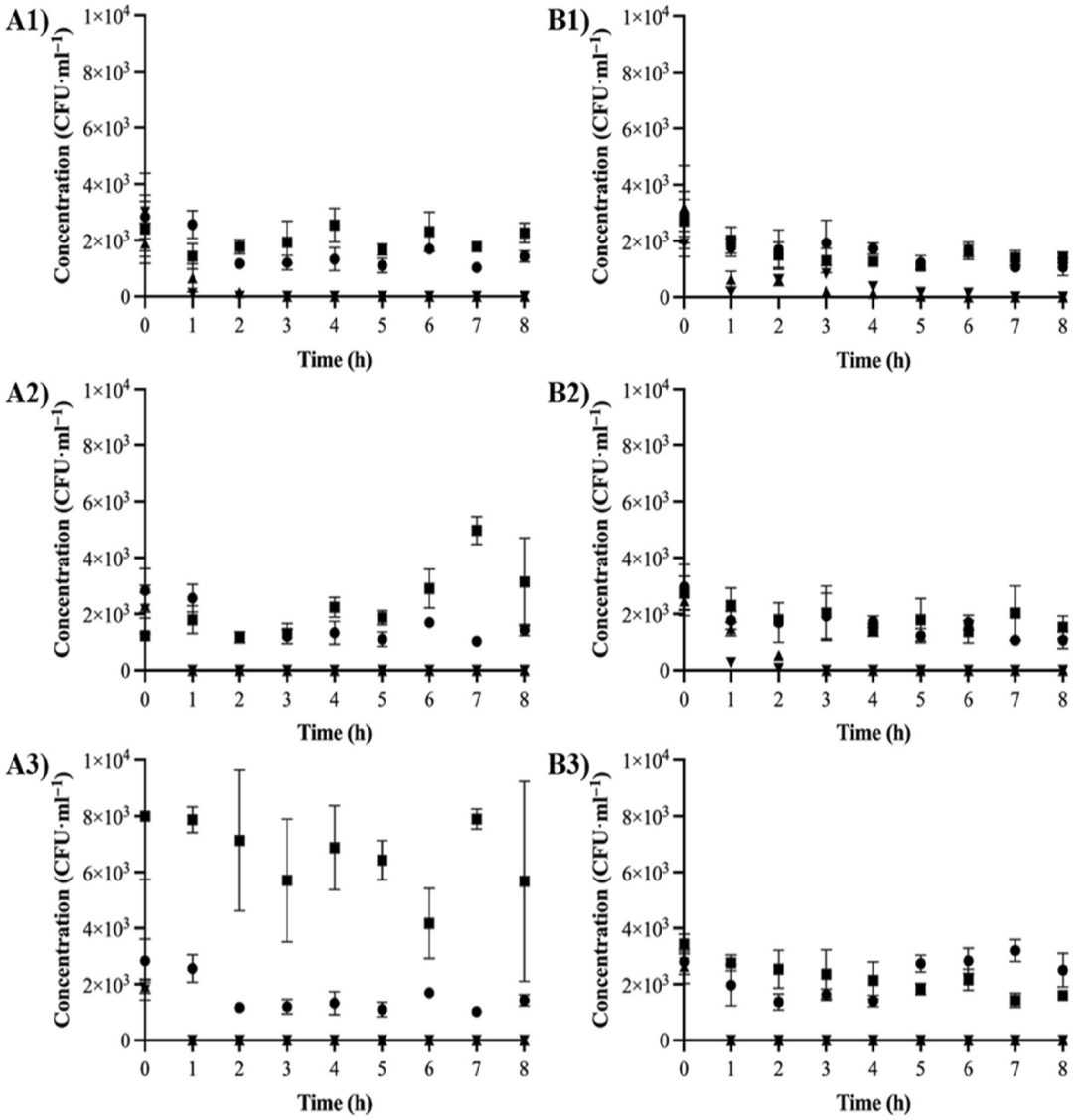

FIGURE 5 | Evaluation of the applicability of the packed bed reactor (PBR) filled to 50% (1), 75% (2), and 100% (3) with glass beads (GB) (●), calcium alginate (CA) (■), $AgNP_{IBCLP20/CA}$ (▲), or $AgNO_{3/CA}$ (▼) for the decontamination of (A) *Escherichia coli* IPT245 and (B) *Pseudomonas aeruginosa* IPT365 at an initial density of 10^3 CFU·mL^{-1}. The reactor was operated at 37°C with a continuous flow rate of 4.0 mL·min^{-1}.

experiment. This is an important parameter for assessing the applicability of $AgNP_{IBCLP20/CA}$, depending on the exposure time of the contaminated water to the nanomaterial encapsulated in CA.

The input densities of the microorganisms tested were 10^3 UFC·mL^{-1}. At a flow rate of 1.0 mL·min^{-1} (Figure 6 A.1), $AgNP_{IBCLP20/CA}$ showed a bactericidal effect against the *E. coli* IPT245 bacterium for practically the entire 8 h of the experiment, with a minimum bacterial survival of 33 UFC·mL^{-1} at the sixth hour of sampling, demonstrating greater antibacterial activity than $AgNO_{3/CA}$, which showed a cell survival of 10^2 UFC·mL^{-1} at the fourth and fifth hours of sampling. With *P. aeruginosa* IPT365 at the same flow rate (1.0 mL·min^{-1}) shown in Figure 6 B.1, the $AgNP_{IBCLP20/CA}$ showed a bactericidal effect after 5 h of operation of the PBR reactor, with cell survival of the bacteria at 10^2 UFC·mL^{-1} in the 1–4 h of sampling and only 33 UFC·mL^{-1} in the 5 h, with the other samplings showing no cell survival.

However, the alginate against *E. coli* IPT245 (Figure 6 A.1) also showed antibacterial activity, reducing the cell density of the bacteria to 10^2 UFC·mL^{-1} from hour 3 to 8 of sampling, unlike *P. aeruginosa* IPT365, which at the same flow rate of 1.0 mL·min^{-1} (Figure 6 B.1) did not show the same pattern when exposed to CA, maintaining cell survival at 10^3 UFC·mL^{-1} throughout the 8 h of the experiment.

The flow rate of 4.0 mL·min^{-1} (Figure 6 A.2 and Figure 6 B.2) maintained the bactericidal effect of both $AgNP_{IBCLP20/CA}$ and $AgNO_{3/CA}$ on the two bacteria. According to Hong et al. (2016) [55], relatively high volumetric flow rates have lower disinfection capacities using nanocomposites, due to the shorter residence time of bacteria with AgNPs, as well as in the study by Wen et al. (2017) [59] which also proved this hypothesis. However, at the highest flow rates tested (7.0 and 10.0 mL·min^{-1}), although the $AgNP_{IBCLP20/CA}$ did not have bactericidal activity over the 8 h of exposure as it did at the flow rate of 4.0 mL·min^{-1}, it still performed better than *P. aeruginosa* IPT365 at the flow rate of

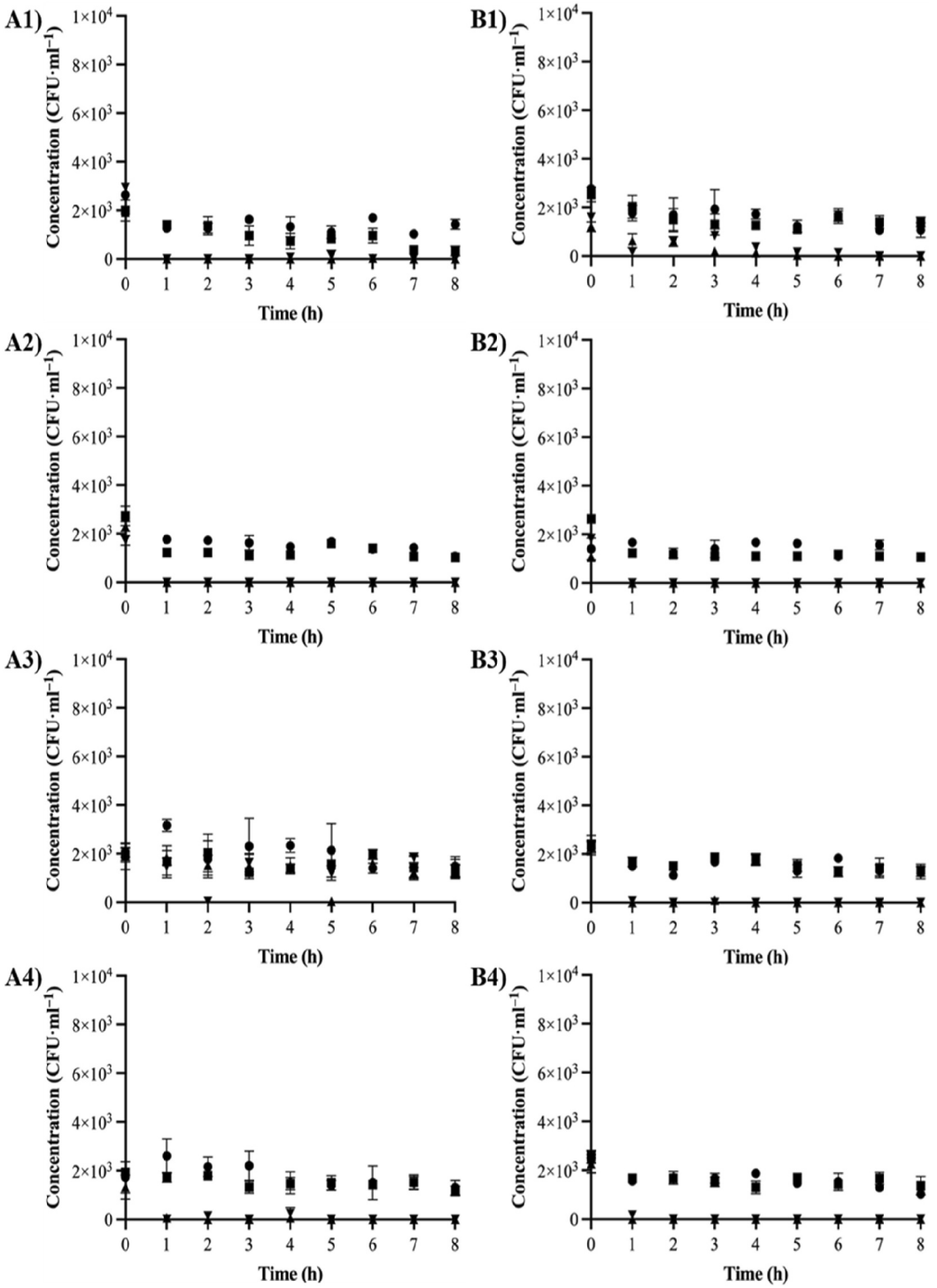

FIGURE 6 | Evaluation of the applicability of the packed bed reactor (PBR) filled to 100% with glass beads (GB) (●), calcium alginate (CA) (■), $AgNP_{IBCLP20/CA}$ (▲), or $AgNO_{3/CA}$ (▼) for the decontamination of (A) *Escherichia coli* IPT245 and (B) *Pseudomonas aeruginosa* at an initial density of 10^3 CFU·mL^{-1}. The reactor was operated at 37°C with a continuous flow rate of 1.0 mL·min^{-1} (1), 4.0 mL·min^{-1} (2), 7.0 mL·min^{-1} (3), and 10.0 mL·min^{-1} (4).

7.0 mL·min^{-1} (Figure 6 B.3), NM had a bactericidal effect in most of the samples, except for 3 h when cell survival of 10^2 CFU·mL^{-1} was observed, unlike IPT245 under the same conditions (Figure 6 A.3) when no bactericidal effect was observed.

However, at a flow rate of 10.0 mL·min^{-1}, $AgNP_{IBCLP20/CA}$ had a greater antibacterial effect against *E. coli* IPT245 (Figure 6 A.4) than *P. aeruginosa* IPT365 (Figure 6 B.4), with cell survival of only 67 UFC·mL^{-1} being observed at hours 1 and 4, as well as 10^3 CFU·mL^{-1} at hour 5, with a bactericidal effect in the other samples taken. This divergence in the antibacterial activity of $AgNP_{IBCLP20/CA}$ may have been due to the existence of dead zones and/or the formation of preferential paths in the reactor at a flow rate of 7.0 mL·min^{-1}, due to the packing of the catalytic bed, leading to a decrease in residence time with the mass of catalyst [60]. When compared

to other studies, such as that of Zarei et al. (2014) [61], who determined a minimum bactericidal concentration (MBC) of 6.25 mg·L^{-1} of Ag $^{+}$ for Gram-negative bacteria at densities of 10^5–10^6 CFU·mL^{-1}, and Li et al. (2010) [62], who indicated that 10 mg·L^{-1} of AgNPs could completely inhibit the survival of 10^7 CFU·mL^{-1} of *E. coli*, it is clear that the available silver concentration in the present study may not have reached the minimum required to achieve a bactericidal effect at higher densities.

Furthermore, Li et al. [63] demonstrated that silver ions have greater antibacterial activity compared to AgNPs, with minimum inhibitory concentrations (MIC) of 0.5 mg·mL^{-1} for *E. coli* and 1 mg·mL^{-1} for *P. aeruginosa* at initial densities of 10^6 CFU·mL^{-1}. Therefore, the applicability of AgNPs depends on several factors such as the morphology of the NP, the concentration of Ag^{+}, flow rate, temperature, and microorganism density [64]. Thus, even though the range used by many studies is 10^5–10^8 CFU·mL^{-1} [52, 55, 57] at higher cellular densities of the microorganism, AgNPs begin to lose their high rate of microorganism survival inhibition, especially against bacteria [64]. Therefore, the use of $AgNP_{IBCLP20/CA}$ in the decontamination of *E. coli* IPT245 and *P. aeruginosa* IPT365 at 10^3 CFU·mL^{-1} is applicable, as the bactericidal effect occurs within 8 h of continuous process operation, and this density is still above the limit imposed by current regulations.

In contaminated waters, the average density of *E. coli* and *P. aeruginosa* can vary significantly, reflecting different levels of pollution and the applicability of treatment systems. According to Ordinance GM/MS No. 888 (Brazilian Ministry of Health, 2021) [65], water supply systems must monitor the presence of *E. coli* monthly. If the moving geometric mean of the last 12 months is equal to or greater than 1×10^3 CFU in 100 mL, it is necessary to evaluate the efficiency of the Water Treatment Plant (WTP) with weekly monitoring of aerobic bacterial spores.

Thus, the choice of a density of 10^3 CFU·mL^{-1} as a fixed value for the parameters evaluated in the PBR reactor is based on the need to ensure that the system is applicable for removing potentially pathogenic bacteria, as required by current regulations. This density serves as a critical reference point to evaluate the applicability of treatment processes and ensure the quality of the treated water, aligning with established standards for public safety and water quality control.

Regarding the volumetric flow rate, the results presented reinforce the hypothesis put forward by Durán et al. [20], suggesting that antimicrobial activity is not solely attributed to silver ions but also to the influence of AgNPs. Additionally, alginate showed bactericidal activity against *E. coli* IPT245 by decreasing the bacterial cell density. This may be due to the extended residence time of *E. coli* IPT245 in contact with the alginate microcapsules, which could have led to microbial aggregation on the encapsulated material. Such aggregation may initiate biofilm formation, facilitated by the biocompatibility and adhesive properties of the immobilizing agent [24, 66, 67], which is a known characteristic of *E. coli*, thereby preventing it from being carried away by the water flow [68].

It is also believed that the low activity values obtained for the continuous reaction system may be related to the low volumetric flow rate in the PBR reactor. Low volumetric flow rates contribute to the formation of a thicker diffusion boundary layer around the particles, making the process limited by external mass transfer. As the volumetric flow rate increases, the boundary layer thickness decreases, favoring the microorganism's access to bio-$AgNP_{AC}$, where the antibacterial activity occurs [5, 69, 70].

3.1.5 | Operational Stability in the Fixed Bed Reactor (PBR)

The evaluation to define the parameters used in the operational stability tests was based on the best parameters from the items described above. The influence of affluent density was proven through the tests carried out, with the lowest density tested (10^3 CFU·mL^{-1}) being the most promising for the best applicability of $AgNP_{IBCLP20/CA}$.

The temperature parameter was the only one that did not show any variation in the bactericidal activity of $AgNP_{IBCLP20/CA}$ and $AgNO_{3/CA}$ at any of the temperatures tested. However, the parameters of catalyst mass and volumetric flow rate showed significant variations, since for large-scale applications one factor is dependent on the other, with higher volumetric flow rates and lower amounts of catalyst mass being more applicable. However, the mass of catalyst that showed the greatest bactericidal activity on the two microorganisms tested, both $AgNP_{IBCLP20/CA}$ and the $AgNO_{3/CA}$ precursor, during the 8 h of the experiment, was 17.5 g (100%).

At the same time, among the volumetric flow rates tested, the highest flow rates (7.0 and 10.0 mL·min^{-1}), despite showing promising results for the antibacterial activity of $AgNP_{IBCLP20/CA}$, only the 4.0 mL·min^{-1} flow rate had bactericidal activity during the 8 h experiment on the two Gram-negative bacteria. Therefore, the volumetric flow rate of 4.0 mL·min^{-1} was considered more promising for the operational stability of the PBR reactor.

Regarding operational stability in the PBR reactor, the results on the influence of influent density are in agreement with studies that state that silver nanoparticles have greater antibacterial activity at densities of 10^3 CFU·mL^{-1} in bacteria [71]. Since the temperature parameter showed no variation in bactericidal activity, the temperature was maintained at 37°C, which is consensus in the literature as the ideal temperature for the survival of *E. coli* and *P. aeruginosa* [47–49, 72] The results of the flow rate study were relevant because, along with the catalyst mass, they influence the residence time. According to Cao et al. [60], this is due to the increased residence time with the compound, which enhances bactericidal activity.

Therefore, the applicability of the PBR reactor was confirmed over an 8-h period, showing operational stability with the following parameters: 10^3 CFU·mL^{-1} and 37°C (microorganism density and temperature); 17.5 g (catalyst mass); and 4.0 mL·min^{-1} volumetric flow rate.

4 | Conclusion

The study demonstrated the applicability and effectiveness of a fixed bed reactor with AgNPs derived from *Aspergillus niger* IBCLP20, encapsulated in calcium alginate ($AgNP_{IBCLP20/CA}$), for the disinfection of contaminated water. The $AgNP_{IBCLP20/CA}$ retained their antibacterial properties even after encapsulation, confirming that the alginate encapsulation is a technique that effectively preserves antimicrobial activity without significantly altering the physicochemical characteristics of the mycogenic AgNPs, both in the colloidal and encapsulated forms.

The analysis of the experimental parameters showed that $AgNP_{IBCLP20/CA}$ exhibit greater toxicity toward the Gram-negative bacterium *E. coli* IPT245 than *P. aeruginosa* IPT365. Nonetheless, promising antibacterial results were obtained for both tested bacteria. Key parameters, such as influent density, temperature, catalyst mass, and volumetric flow rate, were found to significantly influence the reactor performance, highlighting the need for process optimization to improve water treatment.

Considering the above, the implementation of the PBR fixed bed reactor with $AgNP_{IBCLP20/CA}$ proved to be a promising and sustainable solution for the disinfection of contaminated water. The preservation of the NPs antibacterial activity after encapsulation and the insights from the analysis of experimental parameters provide a solid foundation for advancing eco-friendly water treatment systems.

Author Contributions

Ana Laura Pires de Oliveira: conceptualization, writing – original draft, methodology, investigation. **Stella Daniels Kovacs:** methodology, investigation, formal analysis, writing – original draft. **Carolina Assis da Silva:** methodology, investigation, formal analysis. **Caterina do Valle Trotta:** methodology, investigation, formal analysis. **Marta Filipa Simões:** methodology, investigation, writing – review and editing. **Rafael Firmani Perna:** conceptualization, formal analysis, methodology, investigation. **Cristiane Angélica Ottoni:** project administration, funding acquisition, writing – review and editing, supervision, conceptualization.

Acknowledgments

The research described in this work was supported by the São Paulo Research Foundation (FAPESP; grant # 2020/12867-2). CAO acknowledges support from the Conselho Nacional de Desenvolvimento Científico e Tecnológico (CNPq; grants #421122/2023-4 and #313031/2025-8). RFP thanks Minas Gerais Research Foundation (FAPEMIG #APQ-00085-21; #BPD-00030-22) and CNPq (grant #404912/2021-4). MFS was supported by the Science and Technology Development Fund (FDCT), Macau SAR, China (Files No. 0033/2024/ITP1 and 002/2024/SKL) and the National Key Research and Development Program of China (Grant No. 2022YFE0204600). CAS acknowledges scholarships financial support from FAPESP #23/08202-3; #22/05716-3, and #22/03562-9. CVT and ALPO acknowledge scholarships financial support from Coordination for the Improvement of Higher Education Personnel (CAPES # 88882.469336/2019-01 and #88887.822485/2023-00). SK thanks the financial support from CNPq scholarship (114290/2023-7).

Conflicts of Interest

The authors declare no conflicts of interest.

References

1. J. Wolf, P. R. Hunter, M. C. Freeman, et al., "Impact of Drinking Water, Sanitation and Handwashing With Soap on Childhood Diarrhoeal Disease: Updated Meta-Analysis and Meta-Regression," *Tropical Medicine and International Health* 23, no. 5 (2018): 508–525, https://doi.org/10.1111/tmi.13051.

2. L. Anversa, R. C. Arantes Stancari, M. Garbelotti, et al., "*Pseudomonas aeruginosa* in Public Water Supply," *Water Practice and Technology* 14, no. 3 (2019): 732–737, https://doi.org/10.2166/wpt.2019.057.

3. T. Mohapatra, V. Kumar, M. Sharma, and P. Ghosh, "Hybrid Fenton Oxidation Processes With Packed Bed or Fluidized Bed Reactor for the Treatment of Organic Pollutants in Wastewater: A Review," *Environmental Engineering Science* 38, no. 6 (2021): 443–457, https://doi.org/10.1089/ees.2020.0070.

4. M. Chafi, S. Akazdam, C. Asrir, et al., "Continuous Fixed Bed Reactor Application for Decolourization of Textile Effluent by Adsorption on NaOH Treated Eggshell," *International Journal of Materials and Textile Engineering* 9, no. 10 (2016): 1242–1248, https://doi.org/10.5281/zenodo.1339009.

5. S. C. Fogler, Elements of Chemical Engineering Reactions. 4, 2012): LTC, 9788120334168.

6. A. O. Yusuf, G. H. Mohamed, R. Al-Sakkaf, et al., "Photocatalytic Degradation of Diclofenac Amide in a fixed-bed Reactor Using TiO2/β-Bi2O3: Process Optimization and Stability Analysis," *Journal of Photochemistry and Photobiology A: Chemistry* 450 (2024): 115470, https://doi.org/10.1016/j.jphotochem.2024.115470.

7. R. Antonelli, G. R. P. Malpass, M. G. C. da Silva, and M. G. A. Vieira, "Fixed-Bed Adsorption of Ciprofloxacin onto Bentonite Clay: Characterization, Mathematical Modeling, and DFT-based Calculations," *Industrial & Engineering Chemistry Research* 60, no. 10 (2021): 4030–4040, https://doi.org/10.1021/acs.iecr.0c05700.

8. C. Chang, Z. Li, S. Rad, L. Gan, J. Dai, and A. Shahab, "Preparation and Application of Nano TiO2 Filmcoated Recycled low-iron Crushed Glass in a Novel packed-bed Photocatalytic Reactor for Efficient Removal of Biodegradable Contaminants," *Environmental Technology & Innovation* 33 (2024): 103541, https://doi.org/10.1016/j.eti.2024.103541.

9. S. Liao, Y. Zhang, X. Pan, et al., "Antibacterial Activity and Mechanism of Silver Nanoparticles Against multidrug-resistant *Pseudomonas aeruginosa*," *International Journal of Nanomedicine* 14 (2019): 1469–1487, https://doi.org/10.2147/IJN.S191340.

10. S. Mumtaz, S. Ali, S. Mumtaz, T. A. Mughal, H. M. Tahir, and H. A. Shakir, "Chitosan Conjugated Silver Nanoparticles: The Versatile Antibacterial Agents," *Polymer Bulletin* 80, no. 5 (2023): 4719–4736, https://doi.org/10.1007/s00289-022-04321-z.

11. C. A. Ottoni, M. F. Simões, S. Fernandes, et al., "Screening of Filamentous Fungi for Antimicrobial Silver Nanoparticles Synthesis," *AMB Express* 7, no. 1 (2017): 1–10, https://doi.org/10.1186/s13568-017-0332-2.

12. B. Ndaba, A. Roopnarain, R. A. M. A. Haripriya, and M. Maaza, "Biosynthesized Metallic Nanoparticles as Fertilizers: An Emerging Precision Agriculture Strategy," *Journal of Integrative Agriculture* 21, no. 5 (2022): 1225–1242, https://doi.org/10.1016/S2095-3119(21)63751-6.

13. C. A. Silva, B. M. Ribeiro, C. do Valle Trotta, et al., "Effects of Mycogenic Silver Nanoparticles on Organisms of Different Trophic Levels," *Chemosphere* 308 (2022): 136540, https://doi.org/10.1016/j.chemosphere.2022.136540.

14. M. Patar, N. S. Moyon, and T. Sinha, "Biogenic Fabrication of Silver Nanoparticles: A Potent and Ideal Candidate for Wastewater Treatment and Water Disinfection," *ChemistrySelect* 7, no. 1 (2022): e202103374, https://doi.org/10.1002/slct.202103374.

15. A. Khan, M. Jain, A. Pandey, et al., "Leveraging the Potential of Silver Nanoparticles-based Materials Towards Sustainable Water

Treatment," *Journal of Environmental Management* 319 (2022): 115675, https://doi.org/10.1016/j.jenvman.2022.115675.

16. S. Neethu, E. K. Radhakrishnan, and M. Jyothis, "Biofabrication of Nanoparticles Using Fungi," *Nanotechnology for Agriculture: Advances for Sustainable Agriculture* (2019): 53–73, https://doi.org/10.1007/978-981-32-9370-0_4.

17. S. Zainab, M. Jadoon, S. Sikandar, and N. Ali, "*Thermomyces Lanuginosus*: A Prospective Thermophilic Fungus for Green Synthesis and Stabilization of Bioagnps Through Glucoamylase," *Materials Chemistry and Physics* 297, no. 2023 (2023): 127442, https://doi.org/10.1016/j.matchemphys.2023.127442.

18. H. Sonawane, D. Shelke, M. Chambhare, et al., "Fungi-Derived Agriculturally Important Nanoparticles and Their Application in Crop Stress management–prospects and Environmental Risks," *Environmental Research* 212 (2022): 113543, https://doi.org/10.1016/j.envres.2022.113543.

19. F. Ameen, A. A. Al-Homaidan, A. Al-Sabri, A. Almansob, and S. AlNAdhari, "Anti-Oxidant, Anti-fungal and Cytotoxic Effects of Silver Nanoparticles Synthesized Using Marine Fungus *Cladosporium halotolerans*," *Applied Nanoscience* 13, no. 1 (2023): 623–631, https://doi.org/10.1007/s13204-021-01874-9.

20. N. Durán, M. Durán, M. B. de Jesus, A. B. Seabra, W. J. Fávaro, and G. Nakazato, "Silver Nanoparticles: A New View on Mechanistic Aspects on Antimicrobial Activity," *Nanomedicine: NMR In Biomedicine* 12, no. 3 (2016): 789–799, https://doi.org/10.1016/j.nano.2015.11.016.

21. N. Tripathi and M. K. Goshisht, "Recent Advances and Mechanistic Insights into Antibacterial Activity, Antibiofilm Activity, and Cytotoxicity of Silver Nanoparticles," *ACS Applied Bio Materials* 5, no. 4 (2022): 1391–1463, https://doi.org/10.1021/acsabm.2c00014.

22. B. J. Arroyo, A. C. Bezerra, L. L. Oliveira, S. J. Arroyo, E. A. de Melo, and A. M. P. Santos, "Antimicrobial Active Edible Coating of Alginate and Chitosan Add Zno Nanoparticles Applied in Guavas (*Psidium guajava* L.)," *Food Chemistry* 309 (2020): 125566, https://doi.org/10.1016/j.foodchem.2019.125566.

23. W. B. Ayinde, W. M. Gitari, M. Munkombwe, A. Samie, and J. A. Smith, "Green Synthesis of AgMgOnHaP Nanoparticles Supported on Chitosan Matrix: Defluoridation and Antibacterial Effects in Groundwater," *Journal of Environmental Chemical Engineering* 8, no. 5 (2020): 104026, https://doi.org/10.1016/j.jece.2020.104026.

24. M. Alavi and M. Rai, "Recent Progress in Nanoformulations of Silver Nanoparticles With Cellulose, Chitosan, and Alginic Acid Biopolymers for Antibacterial Applications," *Applied Microbiology and Biotechnology* 103, no. 21–22 (2019): 8669–8676, https://doi.org/10.1007/s00253-019-10126-4.

25. A. Pereira, J. L. Fraga, M. M. Diniz, G. C. Fontes-Sant'Ana, and P. F. F. Amaral, "High Catalytic Activity of Lipase From *Yarrowia lipolytica* Immobilized by Microencapsulation," *International Journal of Molecular Sciences* 19, no. 11 (2018): 3393, https://doi.org/10.3390/ijms19113393.

26. M. C. P. Gonçalves, S. A. Morales, E. S. Silva, A. E. Maiorano, R. F. Perna, and T. G. Kieckbusch, "Entrapment of Glutaraldehyde-Crosslinked Cells From *Aspergillus oryzae* IPT-301 in Calcium Alginate for High Transfructosylation Activity," *Journal of Chemical Technology and Biotechnology* 95, no. 9 (2020): 2473–2482, https://doi.org/10.1002/jctb.6429.

27. USEPA, *EPA-821-R-02-013: Short-Term Methods for Estimating the Chronic Toxicity of Effluents and Receiving Waters to Freshwater Organisms* (U. S. Environmental Protection Agency, Office of Water, 2002),335.

28. K. Loza, M. Heggen, and M. Epple, "Synthesis, Structure, Properties, and Applications of Bimetallic Nanoparticles of Noble Metals," *Advanced Functional Materials* 30, no. 21 (2020): 1909260, https://doi.org/10.1002/adfm.201909260.

29. H. T. Phan and A. J. Haes, "What Does Nanoparticle Stability Mean?," *Journal of Physical Chemistry C* 123, no. 27 (2019): 16495–16507, https://doi.org/10.1021/acs.jpcc.9b00913.

30. M. Sardar and J. A. Mazumder, "Biomolecules Assisted Synthesis of Metal Nanoparticles," *Environmental Nanotechnology* 2 (2011): 1–23, https://doi.org/10.1007/978-3-319-98708-8_1.

31. J. A. Mazumder, M. Perwez, R. Noori, and M. Sardar, "Development of Sustainable and Reusable Silver nanoparticle-coated Glass for the Treatment of Contaminated Water," *Environmental Science and Pollution Research* 26, no. 22 (2019): 23070–23081, https://doi.org/10.1007/s11356-019-05647-4.

32. A. Bolewski, M. Matosz, W. Pohorecki, and J. M. del Hoyo-Meléndez, "Comparison of Neutron Activation Analysis (NAA) and Energy Dispersive X-ray Fluorescence (XRF) Spectrometry for the Non-destructive Analysis of Coins Minted Under the Early Piast Dynasty," *Radiation Physics and Chemistry* 171, no. 2020 (2020): 108699, https://doi.org/10.1016/j.radphyschem.2020.108699.

33. M. Khan, M. S. A. Khan, K. K. Borah, Y. Goswami, K. R. Hakeem, and I. Chakrabartty, "The Potential Exposure and Hazards of Metal-based Nanoparticles on Plants and Environment, With Special Emphasis on ZnO NPs, TiO_2 NPs, and AgNPs: A Review," *Environmental Advances* 6, no. 2021 (2021): 100128, https://doi.org/10.1016/j.envadv.2021.100128.

34. S. Agnihotri, S. Mukherji, and S. Mukherji, "Impact of Background Water Quality on Disinfection Performance and Silver Release of Immobilized Silver Nanoparticles: Modeling Disinfection Kinetics, Bactericidal Mechanism and Aggregation Behavior," *Chemical Engineering Journal* 372 (2019): 684–696, https://doi.org/10.1016/j.cej.2019.04.186.

35. C. A. Ottoni, M. L. Neto, P. Léo, B. D. Ortolan, E. Barbieri, and A. O. de Souza, "Environmental Impact of Biogenic Silver Nanoparticles in Soil and Aquatic Organisms," *Chemosphere* 239 (2020): 124698, https://doi.org/10.1016/j.chemosphere.2019.124698.

36. R. Rajan, P. Huo, K. Chandran, B. M. Dakshinamoorthi, S. Yun, and B. Liu, "A Review on the Toxicity of Silver Nanoparticles Against Different Biosystems," *Chemosphere* 292 (2022): 133397, https://doi.org/10.1016/j.chemosphere.2021.133397.

37. S. H. Ching, N. Bansal, and B. Bhandari, "Alginate Gel particles–A Review of Production Techniques and Physical Properties," *Critical Reviews in Food Science and Nutrition* 57, no. 6 (2017): 1133–1152, https://doi.org/10.1080/10408398.2014.965773.

38. S. Kumar, G. Bhanjana, A. Sharma, M. C. Sidhu, and N. Dilbaghi, "Synthesis, Characterization and on Field Evaluation of Pesticide Loaded Sodium Alginate Nanoparticles," *Carbohydrate Polymers* 101 (2014): 1061–1067, https://doi.org/10.1016/j.carbpol.2013.10.025.

39. H. Al-Momani, M. Almasri, D. A. Al Balawi, et al., "The Efficacy of Biosynthesized Silver Nanoparticles Against *Pseudomonas aeruginosa* Isolates From Cystic Fibrosis Patients," *Scientific Reports* 13, no. 1 (2023): 8876, https://doi.org/10.1038/s41598-023-35919-6.

40. M. Azimzadeh, G. Greco, A. Farmani, et al., "Biofilm Inhibition of multidrug-resistant *Pseudomonas aeruginosa* Using green-synthesized Silver Nanoparticles and Colistin," *Scientific Reports* 15, no. 1 (2025): 14993, https://doi.org/10.1038/s41598-025-00005-6.

41. P. Otite Lucky and J. Kusi, "Silver Nanoparticle-Induced Antimicrobial Resistance in *Pseudomonas aeruginosa* and *Salmonella* spp. Isolates From an Urban Lake," *Environmental Pollution* 368 (2025): 125758, https://doi.org/10.1016/j.envpol.2025.125758.

42. M. T. T. Thi, D. Wibowo, and B. H. Rehm, "*Pseudomonas aeruginosa* Biofilms," *International Journal of Molecular Sciences* 21, no. 22 (2020): 8671, https://doi.org/10.3390/ijms21228671.

43. A. Vetrivel, M. Ramasamy, P. Vetrivel, et al., "*Pseudomonas aeruginosa* Biofilm Formation and Its Control," *Biologics* 1, no. 3 (2021): 312–336, https://doi.org/10.3390/biologics1030019.

44. G. Kassab, M. Halalsheh, A. Klapwijk, M. Fayyad, and J. B. Van Lier, "Sequential anaerobic–aerobic Treatment for Domestic Wastewater–A Review," *Bioresource Technology* 101, no. 10 (2010): 3299–3310, https://doi.org/10.1016/j.biortech.2009.12.039.

45. G. F. Alotaibi and M. A. Bukhari, "Factors Influencing Bacterial Biofilm Formation and Development," *American Journal of Biomedical Science & Research* 12, no. 6 (2021): 617–626, https://doi.org/10.34297/AJBSR.2021.12.001820.

46. Ç. Kıvılcımdan Moral and M. Yıldız, "Alginate Production From Alternative Carbon Sources and Use of Polymer Based Adsorbent in Heavy Metal Removal," *International Journal of Polymer Science* 2016, no. 1 (2016): 7109825–7109828, https://doi.org/10.1155/2016/7109825.

47. T. K. Ohshima, K. Okuyama, and M. Sato, "Effect of Culture Temperature on high-voltage Pulse Sterilization of *Escherichia Coli*"," *Journal of Electrostastics* 55, no. 3–4 (2002): 227–235, https://doi.org/10.1016/S0304-3886(01)00206-6.

48. A. K. Bhardwaj, S. Sundaram, K. K. Yadav, and A. L. Srivastav, "An Overview of Silver nano-particles as Promising Materials for Water Disinfection," *Environmental Technology & Innovation* 23 (2021): 101721, https://doi.org/10.1016/j.eti.2021.101721.

49. S. Moon, S. Ham, J. Jeong, H. Ku, H. Kim, and C. Lee, "Temperature Matters: Bacterial Response to Temperature Change," *Journal of Microbiology* 61, no. 3 (2023): 343–357, https://doi.org/10.1007/s12275-023-00031-x.

50. M. A. Tartanson, L. Soussan, M. Rivallin, et al., "A New Silver Based Composite Material for SPA Water Disinfection," *Water Research* 63 (2014): 135–146, https://doi.org/10.1016/j.watres.2014.06.019.

51. B. Song, C. Zhang, G. Zeng, J. Gong, Y. Chang, and Y. Jiang, "Antibacterial Properties and Mechanism of Graphene oxide-silver Nanocomposites as Bactericidal Agents for Water Disinfection," *Archives of Biochemistry and Biophysics* 604 (2016): 167–176, https://doi.org/10.1016/j.abb.2016.04.018.

52. H. Z. Zhang, C. Zhang, G. M. Zeng, J. L. Gong, X. M. Ou, and S. Y. Huan, "Easily Separated Silver nanoparticle-decorated Magnetic Graphene Oxide: Synthesis and High Antibacterial Activity," *Journal of Colloid and Interface Science* 471 (2016): 94–102, https://doi.org/10.1016/j.jcis.2016.03.015.

53. T. Oe, D. Dechojarassri, S. Kakinoki, H. Kawasaki, T. Furuike, and H. Tamura, "Microwave-Assisted Incorporation of AgNP into chitosan–alginate Hydrogels for Antimicrobial Applications," *Journal of Functional Biomaterials* 14, no. 4 (2023): 199, https://doi.org/10.3390/jfb14040199.

54. A. H. El-Aassar, M. M. Said, A. M. Abdel-Gawad, and H. A. Shawky, "Using Silver Nanoparticles Coated on Activated Carbon Granules in Columns for Microbiological Pollutants Water Disinfection in Abu Rawash Area, Great Cairo, Egypt," *Australian Journal of Basic and Applied Sciences* 7, no. 1 (2013): 422–432.

55. X. Hong, J. Wen, X. Xiong, and Y. Hu, "Silver nanowire-carbon Fiber Cloth Nanocomposites Synthesized by UV Curing Adhesive for Electrochemical point-of-use Water Disinfection," *Chemosphere* 154 (2016): 537–545, https://doi.org/10.1016/j.chemosphere.2016.04.013.

56. A. Roy, B. S. Butola, and M. Joshi, "Synthesis, Characterization and Antibacterial Properties of Novel nano-silver Loaded Acid Activated Montmorillonite," *Applied Clay Science* 146 (2017): 278–285, https://doi.org/10.1016/j.clay.2017.05.043.

57. X. Tan, C. Chen, Y. Hu, et al., "Novel AgNWs-PAN/TPU Membrane for point-of-use Drinking Water Electrochemical Disinfection," *Science of the Total Environment* 637 (2018): 408–417, https://doi.org/10.1016/j.scitotenv.2018.05.012.

58. D. Doganay, A. Kanicioglu, S. Coskun, G. Akca, and H. E. Unalan, "Silver-Nanowire-Modified Fabrics for wide-spectrum Antimicrobial Applications," *Journal of Materials Research* 34, no. 4 (2019): 500–509, https://doi.org/10.1557/jmr.2018.467.

59. J. Wen, X. Tan, Y. Hu, Q. Guo, and X. Hong, "Filtration and Electrochemical Disinfection Performance of PAN/PANI/AgNWs-CC Composite Nanofiber Membrane," *Environmental Science and Technology* 51, no. 11 (2017): 6395–6403, https://doi.org/10.1021/acs.est.6b06290.

60. Q. Cao, L. Sang, J. Tu, et al., "Rapid Degradation of Refractory Organic Pollutants by Continuous Ozonation in a Micro-packed Bed Reactor," *Chemosphere* 270 (2021): 128621, https://doi.org/10.1016/j.chemosphere.2020.128621.

61. M. Zarei, A. Jamnejad, and E. Khajehali, "Antibacterial Effect of Silver Nanoparticles Against Four Foodborne Pathogens," *Jundishapur Journal of Microbiology* 7, no. 1 (2014): e8720, https://doi.org/10.5812/jjm.8720.

62. W. R. Li, X. B. Xie, Q. S. Shi, H. Y. Zeng, Y. S. Ou-Yang, and Y. B. Chen, "Antibacterial Activity and Mechanism of Silver Nanoparticles on *Escherichia coli*," *Applied Microbiology and Biotechnology* 85, no. 4 (2010): 1115–1122, https://doi.org/10.1007/s00253-009-2159-5.

63. W. R. Li, T. L. Sun, S. L. Zhou, et al., "A Comparative Analysis of Antibacterial Activity, Dynamics, and Effects of Silver Ions and Silver Nanoparticles Against Four Bacterial Strains," *International Biodeterioration & Biodegradation* 123 (2017): 304–310, https://doi.org/10.1016/j.ibiod.2017.07.015.

64. E. Bahcelioglu, H. E. Unalan, and T. H. Erguder, "Silver-Based Nanomaterials: A Critical Review on Factors Affecting Water Disinfection Performance and Silver Release," *Critical Reviews in Environmental Science and Technology* 51, no. 20 (2020): 2389–2423, https://doi.org/10.1080/10643389.2020.1784666.

65. Brasil Ministério da Saúde, Portaria GM/MS N° 888, De 4 De maio de 2021. Procedimentos de controle e de vigilância da qualidade da água para consumo humano e seu padrão de potabilidade, (2021).

66. L. J. Halverson, "Role of Alginate in Bacterial Biofilms," in *Alginates: Biology and Applications Microbiology Monographs*. 13 (Springer, 2009): 135–151, https://doi.org/10.1007/978-3-540-92679-5_6.

67. G. Sharma, S. Sharma, P. Sharma, et al., "*Escherichia coli* Biofilm: Development and Therapeutic Strategies," *Journal of Applied Microbiology* 121, no. 2 (2016): 309–319, https://doi.org/10.1111/jam.13078.

68. N. Rabin, Y. Zheng, C. Opoku-Temeng, Y. Du, E. Bonsu, and H. O. Sintim, "Biofilm Formation Mechanisms and Targets for Developing Antibiofilm Agents," *Future Medicinal Chemistry* 7, no. 4 (2015): 493–512, https://doi.org/10.4155/fmc.15.6.

69. G. S. Dias, E. D. Santos, M. C. A. Xavier, et al., "Study on the Transfructosylation Activity of *Aspergillus oryzae* IPT-301 Cells in a Packed Bed Reactor Aiming at Fructooligosaccharide Production," *Journal of Chemical Technology and Biotechnology* 97, no. 10 (2022): 2904–2911, https://doi.org/10.1002/jctb.7163.

70. B. M. Ribeiro, L. R. de Sandre Junior, G. de Souza Dias, et al., "Crosslinked Whole Cells for the Sucrose Transfructosylation Reaction in a Continuous Reactor," *Chemical Industry and Chemical Engineering Quarterly* (2023): 15, https://doi.org/10.2298/CICEQ221220015M.

71. S. Bharti, S. Mukherji, and S. Mukherji, "Water Disinfection Using Fixed Bed Reactors Packed With Silver Nanoparticle Immobilized Glass Capillary Tubes," *Science of the Total Environment* 689 (2019): 991–1000, https://doi.org/10.1016/j.scitotenv.2019.06.482.

72. C. R. Chilakamarry, A. M. Mimi Sakinah, A. W. Zularism, I. A. Khilji, and S. Kumarasamy, "Glycerol Waste to Bio-Ethanol: Optimization of Fermentation Parameters by the Taguchi Method," *Journal of Chemistry* 2022, no. 1 (2022): 4892992, https://doi.org/10.1155/2022/4892992.